



Steric exclusion chromatography of lentiviral vectors using hydrophilic cellulose membranes

Jennifer J. Labisch^{a,b,*}, Meriem Kassar^{a,c}, Franziska Bollmann^d, Angela Valentis^c, Jürgen Hubbuch^c, Karl Pflanz^a

^a Lab Essentials Applications Development, Sartorius Stedim Biotech GmbH, Göttingen, Lower Saxony, Germany

^b Institute of Technical Chemistry, Leibniz University Hannover, Hanover, Lower Saxony, Germany

^c Karlsruhe Institute of Technology, Institute of Process Engineering and Life Sciences, Biomolecular Separation Engineering, Karlsruhe, Baden-Württemberg, Germany

^d Marketing Separation Technologies, Sartorius Stedim Biotech GmbH, Göttingen, Lower Saxony, Germany

ARTICLE INFO

Article history:

Received 23 February 2022

Revised 11 May 2022

Accepted 12 May 2022

Available online 14 May 2022

Keywords:

Steric exclusion chromatography

Lentiviral vector purification

Polyethylene glycol

Depletion potential

ABSTRACT

Enveloped viral vectors like lentiviral vectors pose purification challenges due to their low stability. A gentle purification method is considered one of the major bottlenecks for lentiviral vector bioprocessing. To overcome these challenges, a promising method is steric exclusion chromatography which has been used to purify a variety of target molecules. In this study, we successfully identified optimal process parameters for steric exclusion chromatography to purify lentiviral vectors. Lentiviral vector particle recoveries and infectious recoveries of 86% and 88%, respectively, were achieved. The process parameters optimal for steric exclusion chromatography were determined as follows: polyethylene glycol with a molecular weight of 4000 Da, a polyethylene glycol concentration of 12.5%, and a flow rate of 7 mL·min⁻¹ using 5 layers of stabilized cellulose membranes as a stationary phase. High protein and dsDNA removal of approximately 80% were obtained. The remaining polyethylene glycol concentration in the eluate was determined. We defined the maximum loading capacity as 7.5 × 10¹² lentiviral particles for the lab device used and provide deeper insights into loading strategies. Furthermore, we determined critical process parameters like pressure. We demonstrated in our experiments that steric exclusion chromatography is a gentle purification method with high potential for fragile enveloped viral vectors as it yields high recoveries while efficiently removing impurities.

© 2022 The Author(s). Published by Elsevier B.V.

This is an open access article under the CC BY license (<http://creativecommons.org/licenses/by/4.0/>)

1. Introduction

Lentiviral vectors (LV) represent one of the three most commonly used viral vectors for gene transfer in gene therapy clinical trials [1] and are the most frequently used viral gene delivery platform for the *ex vivo* generation of chimeric antigen receptor (CAR)-T cells for cancer immunotherapies [2]. The LV size offers a high genetic cargo capacity. The demand for efficient LV bioprocessing is steadily increasing, incentivizing the development of suitable materials and process strategies for fragile enveloped viral vectors like LV. Downstream processing (DSP) poses many challenges since the transfer of methods developed for protein bioprocessing is unlikely due to the distinct bio- and physicochemical

properties of the molecules. The purification step is considered one of the major bottlenecks for enveloped viral vectors [3,4].

Various chromatographic methods have been utilized for LV purification, such as anion exchange chromatography (AEX) [5–9], heparin affinity chromatography (AC) [10–12], immobilized metal affinity chromatography (IMAC) [12–15], and biotin-streptavidin AC [16,17]. Although promising, these methods have some disadvantages for the purification of enveloped viral vectors. The most widely used chromatographic mode for LV is AEX since it is a simple and cost-effective method. However, elution is performed either by changing the pH or by increasing the ionic strength of the elution buffer. Both treatments result in a decrease in the infectivity of LVs due to their susceptibility to high salt concentrations and to their narrow optimal pH range [4,10,18,19]. Heparin AC is performed under mild conditions; however, selectivity is rather low because DNA and many host cell proteins (HCPs) have an affinity for heparin resulting in a co-elution [4]. In addition to the high costs associated with the resin, heparin presents a major drawback

* Corresponding author at: Lab Essentials Applications Development, Sartorius Stedim Biotech GmbH, Göttingen, Lower Saxony, Germany.

E-mail address: jennifer.labisch@sartorius.com (J.J. Labisch).

since it requires an additional step to eliminate the leaked ligand. This is another issue to consider for the purification of a product intended for clinical use [20]. The desorption reagents required for other affinity chromatography methods, such as guanidine-HCl, D-biotin, and urea for IMAC, imidazole, or ethylenediaminetetraacetic acid (EDTA) for biotin-streptavidin AC, were reported to inactivate the LV [13,21]. Additionally, leakage of metal ions from the matrix and toxicity of desorption reagents are potential hazards and must be considered when LVs are used in clinical trials [22].

For enveloped viral vectors, a potential alternative to commonly performed chromatography methods is steric exclusion chromatography (SXC) as this method does not require any chemical interaction between the target species and the stationary phase. This allows for milder elution conditions and preserves viral activity. SXC was first described by Lee et al. [23] for purifying immunoglobulin M and bacteriophage M13K07 with OH-monoliths, and by Gagnon et al. [24] for purifying IgG on starch-coated magnetic nanoparticles. The application of cellulose membranes as stationary phases for SXC was first published by Marichal-Gallardo et al. [25]. SXC has been proven to effectively purify a variety of viruses: baculovirus [26], Orf virus [27], adeno-associated virus (AAV) [28], and influenza A virus [25]. Typically, screening of a suitable PEG size and concentration needs to be performed for every target molecule. Wang et al. [29] observed increasing retention of their molecule of interest, γ -globulin, by increasing the PEG 6000 concentration from 10% to 15% using a polyacrylamide cryogel monolith as a stationary phase. Marichal-Gallardo et al. [25] purified influenza A with SXC using 8% PEG 6000 and achieved a recovery of 83%. Lothert et al. [30] achieved the highest recovery of above 90% of Orf virus with 8% PEG 8000.

The SXC method principle is shown in Fig. 1A. The mechanism of SXC relies on the depletion potential, which was described by Asakura and Oosawa [31] and further investigated by Vrij [32]. Polyethylene glycol (PEG) molecules are arranged in a random coil structure that can be seen as penetrable hard spheres. When PEG is added to a solution containing viral particles, depletion zones are formed around the viral vectors and adjacent to the hydrophilic stationary phase. The depletion zone is an area that is not accessible to the polymer's center of gravity; hence, the PEG molecules are sterically excluded from this area. This leads to a loss of conformational entropy of the polymer chains that creates a thermodynamically unfavorable increase in free energy that promotes a physical reorganization of the viral vectors. When a viral particle approaches another viral particle (or the stationary phase), the PEG molecules cannot penetrate the gap. Thus, a negative osmotic pressure is created, causing the solvent to flow out between two viral particles (or between a viral particle and the stationary phase) and resulting in weak attraction. When the depletion zones of two viral particles (or of the viral particle and the stationary phase) overlap, the total excluded volume is reduced [33,34]. Excess water is transferred from the PEG-deficient zones to the bulk solvent, reducing the PEG concentration in the bulk solvent, which in turn, decreases the free energy [23]. In a dilute polymer solution, the polymer chains do not interact with one another and the interaction potential depends on the polymer concentration and polymer size, more specifically the gyration radius [35]. The optimal PEG size and concentration depend on the size of the target molecule to be purified. The viral particles are eluted with a buffer that does not contain PEG. The use of PEG-free buffer reserves the association of the viral particles with the membrane, eluting the particles as a result. Mild elution buffers are chosen in which fragile viruses are stable.

In this study, we initially describe how to use SXC for the purification of LVs, defining the optimal PEG size and concentration, as well as the optimal flow rate and maximum loading capacity.

Moreover, we analyze different loading strategies to provide deeper insights into critical process parameters.

2. Materials and methods

2.1. Lentiviral vector production, harvest, and clarification

Third generation lentiviral vectors, which carry a CD19-CAR transgene, were produced by transient transfection of suspension HEK293T/17 SF cells (ACS-4500, ATCC) with four plasmids (Aldenvron) in a UniVessel® 2 L single-use bioreactor (Sartorius). Lentiviral vector production, harvest, and nucleic acid digestion with all materials used are described in detail in Labisch et al. [36]. The lentiviral vector containing cell culture broth was directly clarified using Sartoclear Dynamics® Lab V50 (0.45 μm polyethersulfone membrane version) with 5 $\text{g}\cdot\text{L}^{-1}$ diatomaceous earth (Sartorius) and a Microsart® e.jet vacuum pump (Sartorius). The lentiviral vector was aliquoted and stored at $-80\text{ }^\circ\text{C}$.

2.2. Steric exclusion chromatography

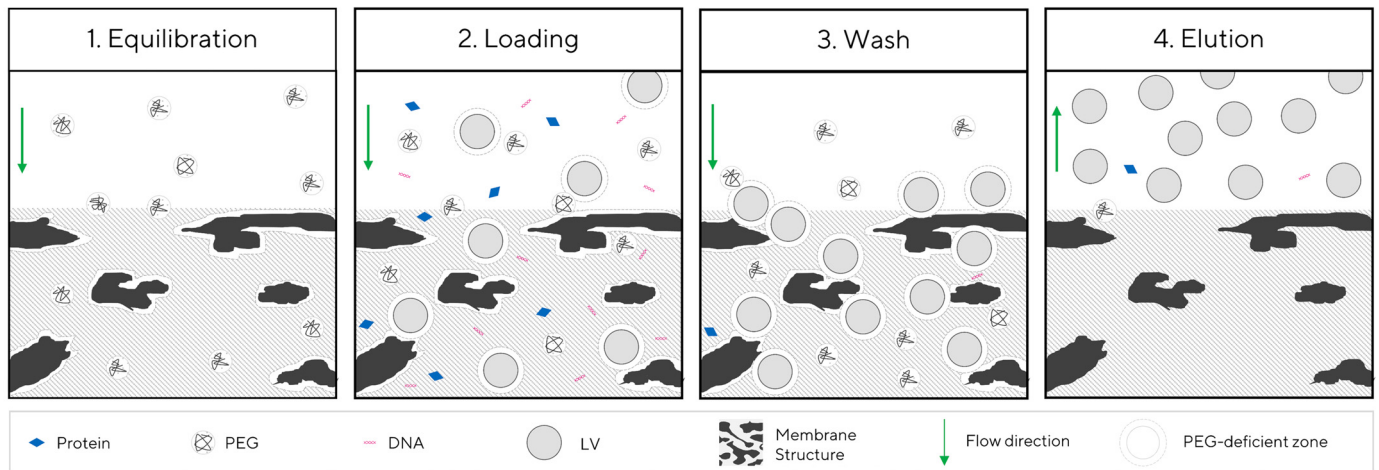
2.2.1. Membrane and housing

A stabilized cellulose membrane Hydrosart® 10242 (Sartorius), a precursor of Sartobind membrane adsorbers, was used as a stationary phase. The porous cellulose membranes are produced in three steps: In the first step, a cellulose acetate membrane is produced from a polymer solution using an evaporation-induced phase separation process. Second, a regenerated cellulose intermediate is made by saponification and, third, the regenerated cellulose intermediate is chemically crosslinked. The membrane is reinforced with a polyester nonwoven. The membrane lot used in this work has a thickness of 230 μm (measured with a thickness gage of 0.01 mm) per layer and a mean flow pore size of 2.5–3 μm (determined with a Porolux 500 porometer). The mean airflow rate at 200 Pa, 20 cm^2 was 17.61 $\text{L}\cdot\text{m}^{-2}\cdot\text{s}^{-1}$ (determined with an air permeability tester FX3300, Textest), and the bubble point was 0.4 bar (determined with automatic filter integrity test system Sartocheck 4 plus, Sartorius). The industrial production of crosslinked cellulose membranes as well as their characterization procedures are described in detail by Tolk [37]. Stacks of 5 or 10 membrane layers with a diameter of 30 mm were incorporated into an MA15 polypropylene module and overmolded with an Arburg 221–75–350 injection molding machine. The final chromatography module has an accessible membrane diameter of 25 mm, resulting in an accessible membrane surface area of 4.91 cm^2 per layer. The MA15 housing is the same as used for the commercial Sartobind® Q 15. The recommended maximum pressure for this device is 0.6 MPa. The integrity of the module is tested by filtering 0.1% charcoal (Carl Roth) in water through the membrane and inspecting the distribution of charcoal on the first layer. Pressures are tested with a static and burst pressure stand (Maximator). Membrane structure was visualized with a Fei Quanta 200 scanning electron microscope. The membrane devices described were used for all experiments in this study.

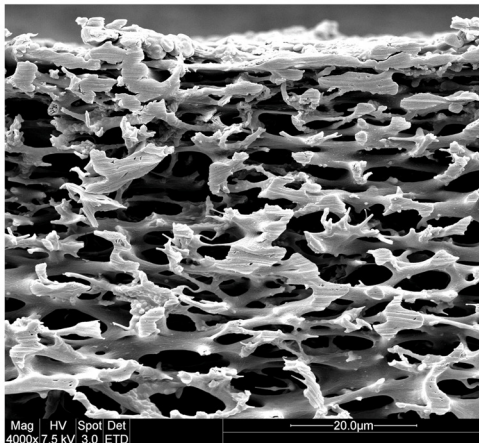
2.2.2. Chromatography setup and procedure

The chromatography system ÄKTA™ avant 150 (Cytiva Life Sciences) with inline UV (280 nm) and conductivity monitoring operated by UNICORN 7.1 software was used for purification of the lentiviral vectors by SXC. Additionally, a multi-angle dynamic light scattering detector (MALS) (Wyatt Technology) connected in-line and operated with Astra 8 software was included for some of the purification runs. The chemicals for the buffers, Tris, hydrochloric acid (HCl), sodium chloride (NaCl), PEG 2000, PEG 4000, and PEG 6000 were purchased by Carl Roth. Buffers were prepared in

A



B



C

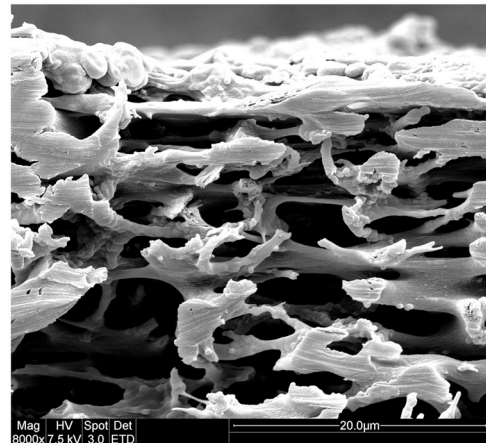


Fig. 1. SXC method principle and stationary phase. A hydrophilic membrane (shown in cross section) is equilibrated with PEG buffer. A PEG-deficient zone forms at the membrane surface, due to the inability of the PEG molecules to fully penetrate this area because of their hydrodynamic radius. During loading a PEG-deficient zone is formed around the LV particles' surface as well (A1). The LV particles associate with the stationary phase, whereas impurities are removed in the flow through (A2). The membrane is then washed with PEG buffer and the LVs remain associated with the stationary phase while unbound remaining impurities are washed out (A3). LVs dissociate from the stationary phase when eluted with Tris buffer (A4). Schematic visualization only; sizes differ in reality: in relation to the pore size, the LV is magnified 10 times and the other molecules (PEG, protein, DNA) are shown magnified 100 times. Exemplary scanning electron microscope pictures of the stabilized cellulose membrane in cross section at 4,000x (B) and 8,000x magnification showing the membrane pore structure of one membrane layer (C).

ultrapure water of Arium® Pro (Sartorius). Two buffers were employed to perform SXC: 1) a 50 mM Tris-HCl buffer with 150 mM NaCl, pH 7.4 (A1), and 2) a PEG buffer with 50 mM Tris-HCl, 150 mM NaCl pH 7.4, and PEG with a certain molecular weight and concentration depending on the experiment conditions (B1). In the following, the buffers are referred to as Tris buffer and PEG buffer.

On the day of the experiment, the LV sample was thawed in a water bath at 37 °C until only small ice clumps remained. The LV sample was then stored at 4 °C until use (30–60 min). The LV solution was used up on the day of thawing. Different LV batches were used for different experiments; therefore, the respective titer of each LV sample is indicated in the results section. The LV solutions were frozen up to 6 months before use. The LV solution was kept on ice during the experiments and the fractions were collected and cooled at 4 °C. The MA15 membrane device was first equilibrated with 20 mL of the Tris buffer and the PEG buffer that were mixed inline at a ½ dilution. For example, a PEG buffer with a concentration of 25% (w/v) PEG 4000 would then equal a final PEG concentration of 12.5%. The loading strategy experiment was

performed with PEG 6000 at a concentration of 10% (Section 3.1). In Section 3.2 the first experiments were conducted to investigate the effect of the PEG concentration on the strength of the depletion attraction using PEG 4000 and PEG 6000 at final concentrations of 7.5%, 10%, and 12.5%. The second experiment of Section 3.2 was conducted to investigate the effect of PEG size on the range of the depletion attraction. Therefore, PEG size was systematically varied using PEG with three molecular weights: PEG 2000 Da, PEG 4000, and PEG 6000, as well as a mixture of PEG 2000 and PEG 4000. All buffers had a final PEG concentration of 12.5%. Further experiments (Section 3.3–3.5) were performed with 12.5% PEG 4000. The PEG molecular weights and concentrations are indicated for each experiment in the results section. The LV sample (A2) was loaded by inline mixing with the PEG buffer at a ½ dilution, if not indicated otherwise. The loading volume varied between experiments and is provided in the results section for each experiment. The membrane column was then washed with 15 mL of Tris buffer and PEG buffer that were mixed inline at a ½ dilution. The LVs were eluted with 20 mL of Tris buffer, if not indicated otherwise. Fractions were aliquoted and stored at –80 °C for analysis. The flow

rates, PEG size, and PEG concentration varied depending on the experiment. A new membrane device was used for every run. All experiments were performed in triplicate.

2.3. Analytics

2.3.1. Infectious titer determination using the Incucyte® S3

The infectious LV titer was quantified using the live-cell analysis system Incucyte® S3 (Sartorius). Adherent HEK293T cells (ACC 635, DSMZ) were infected with serially diluted LV samples, and the expression of the CD19-CAR was measured by an immunological real-time imaging method. The method and materials used are described in detail in Labisch et al. [19].

2.3.2. Particle titer determination with p24 ELISA

The LV particle titer was quantified by performing a p24 enzyme-linked immunosorbent assay (ELISA) using the QuickTiter™ Lentivirus titer kit (Cell Biolabs). The absorbance was read at 450 nm with a FLUOstar Omega plate reader (BMG Labtech). The absorbance at 450 nm of the samples correlated with the concentration of the p24 capsid protein. The standard curve obtained was fitted by a second-degree polynomial. The p24 concentrations determined were converted into viral particle titers by assuming that 1.25×10^7 LV particles contain 1 ng of p24 and 1 LV particle contains about 2000 molecules of p24 [38].

2.3.3. Total protein quantification

The total protein concentration was determined with the Pierce™ Coomassie Bradford protein assay kit (Thermo Fisher Scientific). The kit was used according to the manufacturer's instructions. Standards and samples were analyzed in duplicates in transparent 96-well microtiter plates (Greiner Bio-one). The absorbance was read at 595 nm with a FLUOstar Omega plate reader. The standard curve obtained was fitted by linear regression.

2.3.4. Total dsDNA quantification

The dsDNA content was determined with the Quant-iT™ PicoGreen™ dsDNA assay (Thermo Fisher Scientific). The assay was performed according to the manufacturer's instructions. Standards and samples were analyzed in duplicates in a 96-well black microplate (Corning). The samples were excited at 480 nm, and the fluorescence emission intensity was measured at 520 nm using the FLUOstar Omega microplate reader. The standard curve obtained was fitted by linear regression.

2.3.5. Determination of the PEG concentration

A modified Dragendorff method was performed to determine the remaining PEG concentration in the elution fractions. A quantity of 0.17 g bismuth subnitrate (Fluka) was dissolved in 2 mL glacial acetic acid (Fluka) in a 20 mL Erlenmeyer flask and diluted to a volume of 20 mL with deionized water (solution A). Four grams of potassium iodide (TCl) was dissolved in 10 mL of deionized water (solution B). Solutions A and B, each in a volume of 5 mL, and 20 mL of glacial acetic acid were added to a 100 mL Erlenmeyer flask and diluted to a volume of 100 mL with deionized water to obtain the Dragendorff reagent. Then 2 g of barium chloride (Fluka) was dissolved in 8 mL of deionized water. PEG 4000 standards in a concentration range from 0.1 to 1 g·L⁻¹ were prepared; 0.5 mL PEG 4000 standards or SXC elution fractions were added to a 1.5 mL reaction tube. Next, 0.1 mL of barium chloride solution, 0.2 mL of Dragendorff reagent, and 0.2 mL of deionized water were added and mixed. Samples were incubated for 15 min. Standards and samples were analyzed in duplicate in transparent 96-well microtiter plates (Greiner Bio-one). The absorbance was read at 510 nm using a plate reader. The standard curve obtained was fitted by linear regression.

2.4. Statistical analysis

The statistical significance of between-group differences was evaluated by using unpaired Student's t-tests (two-tailed) with OriginPro® 2021 (OriginLab). Where applicable, experiments were evaluated with MODDE Pro 13 (Sartorius). Results are presented as mean ± standard deviation of triplicates.

3. Results and discussion

3.1. Impact of mixing shear and buffer systems on LV infectivity as well as of a suitable LV loading strategy

SXC is considered a milder chromatography method for enveloped viral vectors compared with AEX or affinity chromatography. To investigate whether the PEG buffer used for SXC has an impact on LV infectivity, an LV solution was mixed in a 1:1 ratio with 25% (w/v) PEG 4000 buffer, resulting in a final PEG concentration of 12.5%. Besides this, LV was incubated with the Tris-HCl elution buffer and the virus production medium FreeStyle293. An LV-free sample served as a negative control. The samples were incubated for 1 h at 4 °C first, then LV infectivity was determined according to Section 2.3.1. The samples were incubated for 1 h since the maximum duration of one SXC run was 35 min and within 1 h the fractions were aliquoted and stored at -80 °C until analysis. The incubation was performed at 4 °C as LV was kept on ice during SXC runs and fractions were cooled at 4 °C before freezing. Further stability data of the LV at different temperatures and incubation times were previously published [19]. The incubation of LV with the PEG buffer or the Tris-HCl buffer did not reduce the infective titer significantly ($p \leq 0.05$) compared to the sample incubated with medium as shown in Fig. 2A. The LV is present in the production medium after harvest and clarification. The medium sample, therefore, serves as a control. We showed that PEG buffer and Tris-HCl buffer do not reduce the biological activity of LV.

To analyze the effect of LV pass-through in the chromatography system on the LV infectivity, several bypass runs were performed. As the LV material needed to be mixed with the PEG buffer before loading, we chose to explore different mixing strategies available: The first option involved mixing the LV solution with PEG buffer externally in a bottle by using a magnetic stirrer with a magnetic stir bar and by loading the ready-mixed solution via the sample valve of the chromatography system. The second option entailed mixing the two solutions internally in the chromatography system using its dynamic mixer. We investigated both strategies with the aim of obtaining high virus recoveries. Moreover, the MALS detector was either connected to or disconnected from the system to further analyze the effect of the additional pressure caused by the detector. The differences in infective titer recoveries of the bypass runs are negligible (Fig. 2B), regardless of whether internal or external mixing was performed. The connection of the MALS detector increased the pressure from 0.21 MPa to 0.38 MPa. When a membrane adsorber is connected, a higher pressure must be considered. All in all, the chromatography system, as well as the dynamic mixer itself, did not have a significant impact on the LV infectious titers, achieving recoveries of 90% or more. A possible explanation could be that the viscosity of the PEG buffer somewhat reduces shear stress, for instance that is generated by the dynamic mixer; therefore, the impact of shear stress might be low. Our observation is consistent with Ruscic et al. [39], who reported no significant LV loss by the fast liquid chromatography system used in their study for ion exchange chromatography.

In a second experiment, the different loading strategies of internal and external mixing as described above were tested by performing SXC. The experiments were carried out using PEG with a molecular weight of 6000 Da at a final concentration of 10% and

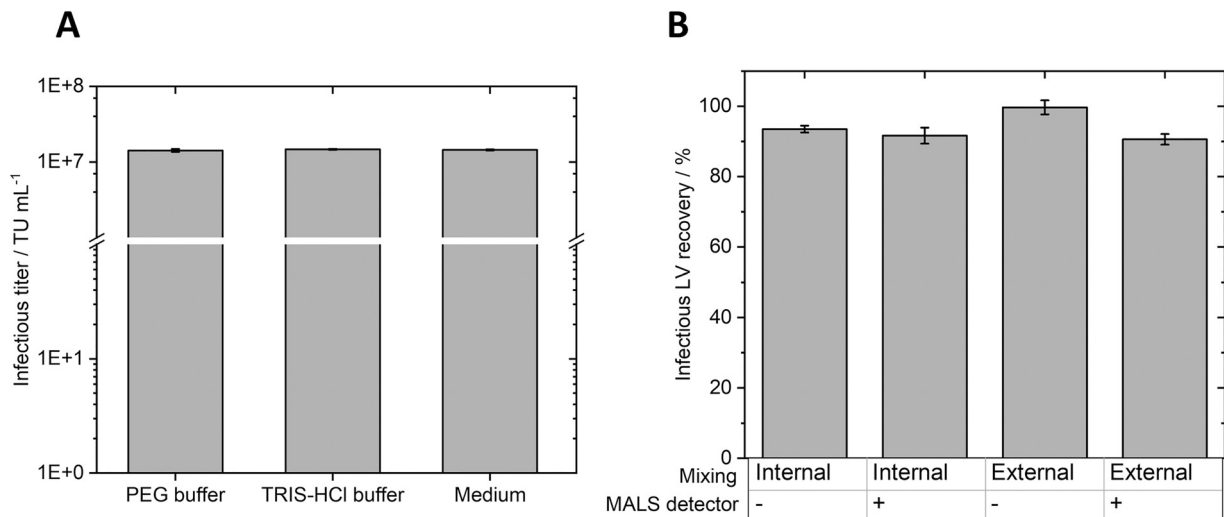


Fig. 2. Shear and buffer impact on LV infectivity. Infectious titers after incubation of LV with different buffers or medium for 1 h at 4 °C (A). Infectious titer recoveries for bypass experiments with the chromatography system and the MALS detector using two different mixing strategies of the LV and the PEG buffer (B).

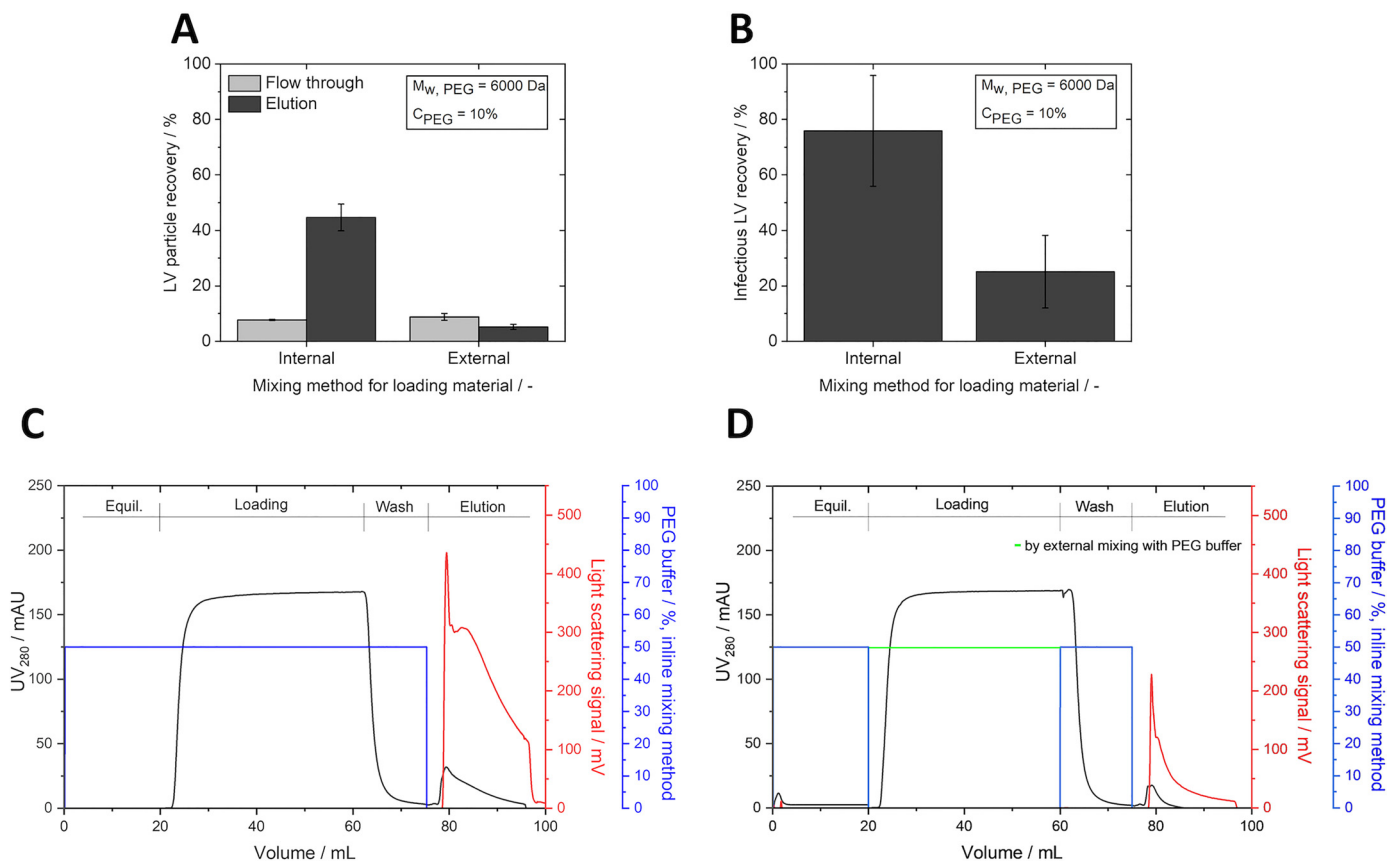


Fig. 3. Comparison of mixing methods for LV loading. LV particle recovery (A) and infectious recovery (B) in the elution fraction of different mixing strategies during the loading step. Chromatograms of SXC runs with internal (C) or external mixing (D) of LVs with PEG buffer. The UV signal is shown in black, the light scattering signal in red; the percentage of PEG buffer added during inline mixing in blue, and during external mixing in green.

a flow rate of 7 mL·min⁻¹. We chose PEG 6000 based on previous publications [23–25,28,40,41] as a starting point to investigate the ideal loading strategy before identifying a suitable PEG size and concentration. Internal mixing resulted in a significantly higher particle recovery ($p \leq 0.001$) of $45 \pm 5\%$ compared with $5 \pm 1\%$ for external mixing of LV with PEG buffer. In the flow through fractions, similar LV particle recoveries of about 8% were detected for both mixing strategies (Fig. 3A). The wash fraction was not plotted since LV particle recovery in the wash fractions was

below or equal to 2% for all runs. The infectious LV recovery for internal mixing was $76 \pm 20\%$, significantly higher ($p \leq 0.05$) than that of $25 \pm 13\%$ for external mixing (Fig. 3B). We did not analyze the infectious titer in the flow through and wash fractions, because only a very small amount of LV particles was recovered in these fractions, and this is difficult to detect by an infectivity assay. First, the volume of the flow through section is large; thus, the LV in the flow through fractions is highly diluted; and second, the p24 detected in the flow through and wash fraction might also be

stem from non-infectious LV debris, resulting in a signal below the detection limit. Two representative chromatograms (Fig. 3C and D) confirm the observation of the titer assays. When internal mixing was performed during loading, the elution peak showed a higher light scattering signal, indicating a larger number of eluted particles compared with the elution peak when the LV was mixed externally and then loaded. When the LV solution is mixed with PEG, the unfavorable excess in free energy caused by the formation of PEG-deficient zones can be either reduced by LV self-association or by the association of LV with the stationary phase. Internal mixing can possibly promote association with the stationary phase because the LV is mixed with PEG shortly before reaching the stationary phase. By contrast, external mixing may lead to LV aggregation since the incubation time is longer before reaching the membrane surface. The formation of aggregates may hinder the subsequent elution of LV particles, resulting in low LV recoveries. These observations are consistent with other studies that reported particle aggregation when adeno-associated viral vectors were mixed with the PEG buffer externally [28]. This phenomenon was first postulated by Lee et al. [23], who performed inline mixing due to a potentially preferred association of the target molecule with the stationary phase, preventing aggregation of the target molecules with one another. On the other hand, external mixing of baculovirus with PEG buffer and loading via a loop has been reported to yield high vector recoveries [26]. Although the preferred use of inline mixing was discussed and reported before, this is the first study presenting comparative data. Based on these findings, all further experiments were performed by mixing the LV with the PEG buffer internally in the chromatography system.

3.2. Optimal PEG size and concentration for LV purification

The aim of this investigation was to determine an optimal PEG size and concentration at which both high LV particle and infectious recoveries, as well as high dsDNA and protein removal, are achieved. The first experiment (Fig. 4) was conducted to investigate the effect of PEG concentration on the strength of the depletion attraction. PEG with molecular weights of 4000 Da and 6000 Da and concentrations of 7.5%, 10.0%, and 12.5% were tested systematically. SXC devices described in Section 2.2.1 with 5 and 10 membrane layers were used. Two different numbers of layers were tested because the surface area required to capture LV successfully was not yet known, or whether a certain number of layers was required to prevent LV breakthrough. LV solution was loaded in the same volumes of 25 mL LV solution for 5-layer and 10-layer membrane devices, corresponding to 6.25×10^{12} total viral particles (2.50×10^{11} VP·mL⁻¹) and 9.25×10^7 infectious viral particles (3.70×10^6 TU·mL⁻¹). The ratio between physical particles compared to functional particles of the product was 6.7×10^4 VP·TU⁻¹. This solution equaled a 50 mL loading volume as the LV was mixed in a dilution of 1/2 with PEG buffer. The percentages of LV particle recovery in the flow through and elution fractions were plotted against the corresponding PEG concentration (Fig. 4A and B). The wash fraction was not plotted since LV particle recovery in the wash fractions was below 3% for all runs.

The LV particle recovery in the elution fractions rose as the PEG 4000 concentration increased (Fig. 4A). For a 5-layer membrane device, only $32 \pm 13\%$ of the LV particles were recovered in the elution fraction at a PEG 4000 concentration of 7.5%, whereas a high percentage of $69 \pm 3\%$ of LV particles were lost in the flow through fraction. For the concentrations of PEG 4000 analyzed we have a dilute concentration regime of the polymer solution. In dilute polymer solutions, the range of depletion attraction depends on the polymer size, while the strength of the interaction depends on the polymer concentration [42]. When PEG 4000 was used at a concentration of 7.5%, the ratio of PEG molecules

to LV particles was too low to achieve the depletion attraction of all LV particles, and a high amount of LV was lost in the flow through fraction. Using a 10-layer membrane resulted in a significantly lower LV loss ($p \leq 0.001$) in the flow through fraction, but recovery in the elution fraction was similar to 7.5% PEG 4000 using an SXC device with 5 membrane layers. One possible reason could be that the critical proximity required between the LV and the membrane is less frequently present with 5 layers. With 10 layers, the LV particles must pass through more membrane layers, which means an increased chance that an LV particle might encounter the membrane, then drop below the critical proximity required to result in capture. Concentrations of 10.0% and 12.5% PEG 4000 yielded significantly higher LV particle recoveries ($p \leq 0.01$) in the elution $72 \pm 7\%$ and $86 \pm 18\%$, respectively, compared with the 7.5% PEG 4000 concentration. Large error bars and recoveries above 100% are often reported when working with lentiviral vectors, or viral vectors in general, with error bars of 20–30% and even higher being reported in recent publications [6,39]. This is attributed to the inherent variability of the titer assays. Moreover, only a small amount of LV was lost in the flow through fraction (1–5%). A higher ratio of PEG molecules to LV particles induced a higher osmotic pressure around the LV particles, resulting in particle attraction. This led to a higher fraction of LV particles retained at the hydrophilic surface of the membrane with increasing PEG 4000 concentration and thus higher LV particles recovered in the elution fraction. A comparable trend is observed when using a 10-layer membrane device. Considering the experimental error there is no significant difference in the recovery of LV particles in the elution fraction when using 5 or 10 membrane layers for all PEG 4000 concentrations tested. No pronounced effect of PEG 6000 concentration on LV particle recovery was observed for the 5-layer membrane device with recoveries in the elution fraction ranging from $38 \pm 6\%$ to $52 \pm 2\%$ (Fig. 4B). When a 10-layer membrane device was used, the highest LV particle recovery of $51 \pm 7\%$ was achieved at a 7.5% PEG 6000 concentration. A further increase in the PEG 6000 concentration led to a significant decrease in LV particle recovery ($p \leq 0.01$) in the elution down to $26 \pm 2\%$. The particle recovery was almost twice as low as the highest recovery obtained with PEG 4000. When PEG 6000 was used at the concentrations investigated, the viscoelastic properties of the PEG buffer started approaching those of a semi-dilute polymer solution as obtained by the scheme of polymer solutions published by Baumgaertel and Willenbacher [43]. This means the PEG molecules begin to interact with one another and the movement of PEG chains is restricted, depending on the movement of another polymer chain [44]. In this regime, the range of depletion attraction is independent of the polymer size, and the strength of the interaction is a decreasing function of the concentration [34]. This may explain the lower LV particle recoveries and an overall higher variability in LV recoveries in previously performed experiments using PEG 6000 (data not shown). When PEG 6000 was used, negligible LV particle recoveries in the flow through fractions were measured, with values below 3% regardless of the number of membrane layers. The PEG-free depletion zone around the LV particle correlates to the PEG size. When PEG 4000 is used at a concentration of 7.5%, the total excluded volume of PEG is lower than when PEG 6000 with the same concentration is used. Therefore, a lower amount of LV particles was lost in the flow through fraction using PEG 6000.

Infectious titer recoveries were not significantly different using different concentrations of PEG 6000 and 5 or 10 membrane layers (Fig. 4D), whereas, for PEG 4000, a similar trend was observed (Fig. 4C), as described for the particle titer. The infectious titer recovery rose significantly ($p \leq 0.01$) from 67% to 84–88% when the PEG 4000 concentration was increased from 7.5% to 10.0% or to 12.5% using 5 membrane layers. Using 10 membrane layers and PEG 4000 at a concentration of 12.5% resulted in a significantly

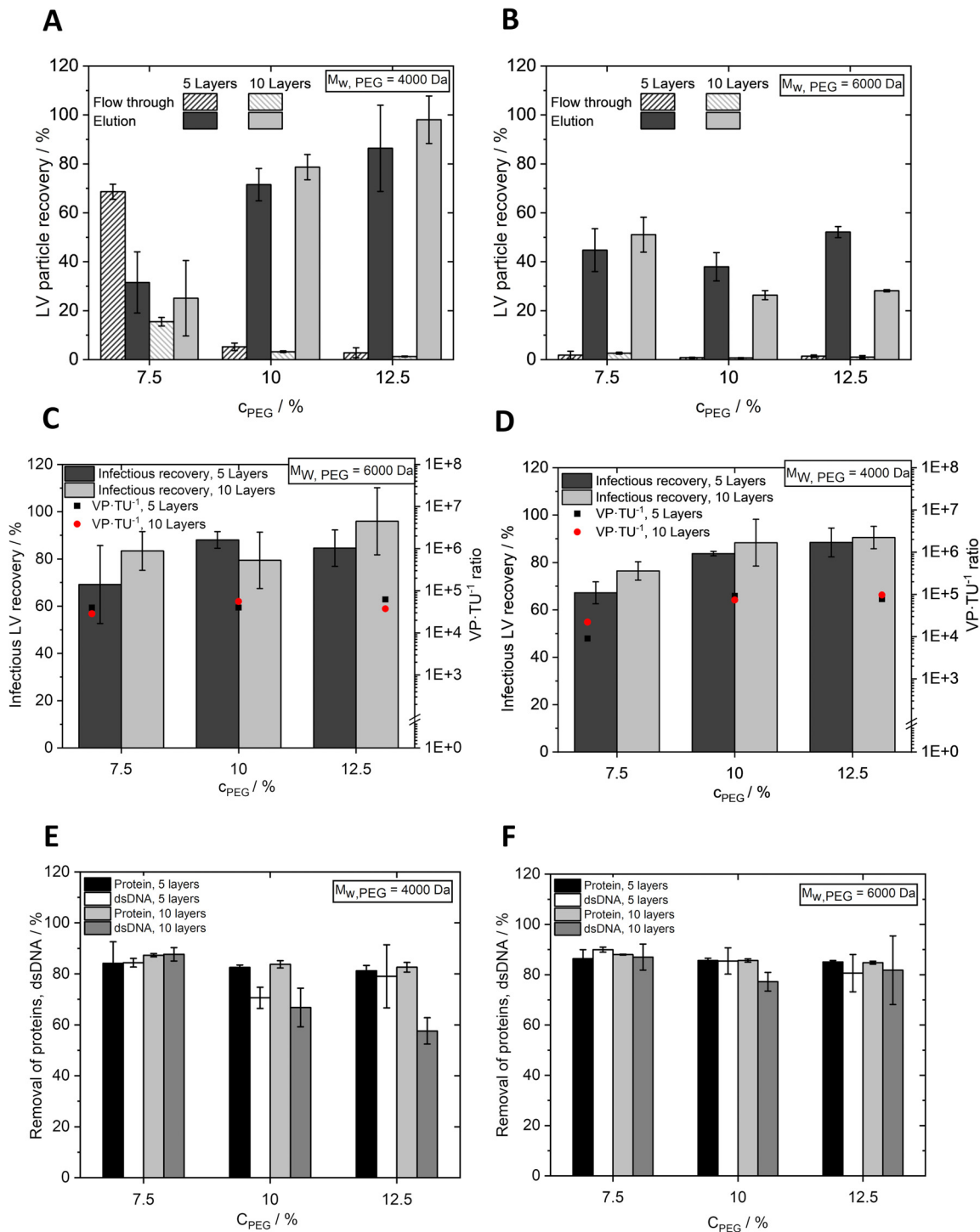


Fig. 4. LV titer recoveries and impurity removal using different PEG sizes and concentrations. LV particle recovery in flow through and elution fractions using PEG with molecular weights of 4000 Da (A) and 6000 Da (B), respectively, plotted against three different PEG concentrations. Infectious LV recovery and viral particle to transducing unit ratio (VP·TU⁻¹) in the elution fraction using PEG with molecular weights of 4000 Da (C) and 6000 Da (D), respectively, plotted against the different PEG concentrations. Protein and dsDNA removal using PEG with molecular weights of 4000 Da (E) and 6000 Da (F), respectively, plotted against the different PEG concentrations. SXC devices with 5 and 10 membrane layers were used.

increased infectious titer recovery ($p \leq 0.05$) compared with a PEG concentration of 7.5% (91% recovery compared with 76%). As above described, a higher ratio of PEG molecules to LV particles increases the strength of depletion attraction, inducing a higher osmotic pressure around the LV particles, resulting in particle attraction. This led to a higher fraction of infectious LV particles retained at the hydrophilic surface of the membrane with increasing PEG 4000 concentration and thus higher infectious LV recovery in the

elution fraction. Contrary to conventional chromatography methods for LV purification, which often significantly reduce the biological activity of enveloped viral vectors [3], SXC provides gentle purification conditions, which is advantageous for fragile enveloped viral vectors. All buffers used during SXC had a pH that preserves LV activity [18] and a low salt concentration that does not reduce LV infectivity [19]. Presumably, PEG may reduce, to some extent, the impact of shear stress applied to LV particles during purification.

According to flow mechanics of non-Newtonian fluids, viscoelastic properties induced by the addition of shear-thickening agents such as polymers hinder the deformation of suspended particles as polymer chains deform [45,46]. Another advantage is that, due to the mild elution conditions for SXC, no additional processing steps after elution are required, such as dilution of the eluate or immediate desalting as performed for AEX [39,47,48]. A recent publication by Valkama et al. reported an LV recovery of 33% with AEX [6]. Other studies performing AEX with LV typically reported recoveries below 60% [3,4]. This outlines the necessity for optimized purification methods for LV and the great potential of SXC that yields LV recoveries above 80%.

The protein and dsDNA removal for PEG 4000 and PEG 6000 at different concentrations were measured and shown in Fig. 4E and 4F. The dsDNA and protein concentrations of the loading material were $321 \text{ ng}\cdot\text{mL}^{-1}$ and $204 \text{ }\mu\text{g}\cdot\text{mL}^{-1}$, respectively. Overall high removal of protein and dsDNA impurities of approximately 80% was observed. The removal of impurities was similar for different PEG sizes and concentrations. The reason for this is discussed in the following: The polymers PEG 2000, 4000, and 6000 have a gyration radius of 1.6 nm, 2.5 nm, and 3.1 nm [44], respectively, and are preferentially excluded from the vicinity of large molecules like LV particles. A typical host cell protein is the heat shock protein 70 [49] which has a hydrodynamic radius of approximately 3.5 nm. During LV production, DNase (DENARASE, c-LEcta) was used to cleave dsDNA into fragments with an expected length of approximately 5–8 bp according to the specifications of the manufacturer. With one base pair being approximately 340 pm long [50], this results in a length of 1.7 nm to 2.7 nm. However, the pronounced size difference between the LV particles (100 nm in diameter) and the contaminants allows selective retention of the larger LV particles. Therefore, nearly none of the small impurities are retained so they are efficiently removed in the flow through fraction. The impurity removal with SXC was 80–90%, which equals a log removal of 0.7 to 1. For AEX DNA removals of greater than 90% were achieved [47,51] and 2-log removal of HCPs and DNA was reported [39]. Although the impurity removal with AEX is higher compared with SXC, the advantage of SXC lies towards the LV recovery of above 80%. For AEX LV recoveries are typically below 60% [3,4,6]. Heparin affinity chromatography of LV removed 94% and 56% of protein and DNA impurities, respectively, while recovering 53% of infectious LV particles [11]. Heparin affinity chromatography yields overall a lower impurity removal and LV recovery compared with SXC. Affinity chromatography yielded a 2-log reduction of host cell DNA and protein impurities, which is higher than for SXC, but recovered only 60% of infectious LV [17]. Moreover, no ligand leaching occurs during SXC because hydrophilic cross-linked cellulose membranes without ligands are used, which eliminates additional purification costs as required for affinity chromatography [20,22]. To evaluate the most suited chromatography technique, not only the impurity removal must be considered, but the virus recovery, as well as other aspects like potential ligand leakage. The favor of SXC over traditional techniques is the high LV recovery in combination with good impurity removal.

An optimal PEG concentration was identified at 12.5% using PEG 4000. Based on this finding, the next experiment was performed to investigate the effect of PEG size on the range of the depletion attraction. Therefore, PEG size was systematically varied using PEG with three molecular weights: one lower than 4000 Da (PEG 2000) and one higher (PEG 6000). The range of the depletion interaction depends on the size of the polymer. It has been hypothesized that a more polydisperse distribution of the molecular weight of the polymers may lead to a higher depletion of the colloidal particles [52]. To analyze this, a PEG buffer with a final concentration of 12.5% was prepared using a mixture of PEG 2000 and PEG 4000 with a molarity ratio of 1:2 and compared

with other monodisperse PEG buffers having the same concentration (Fig. 5A and B). A mixture of PEG 4000 and PEG 6000 was not tested as this buffer has a higher viscosity that in turn leads to a higher pressure compared with a monodisperse PEG 4000 buffer. Therefore, we tested a mixture of PEG 4000 with a lower molecular weight PEG to investigate if the performance is comparable to the monodisperse PEG 4000 buffer and at the same time resulting in a lower pressure (Fig. 7A) that is advantageous for the process as discussed in more detail in Section 3.4. For this experiment, another LV batch was used as for the previous experiments. The flow rate was set to $7 \text{ mL}\cdot\text{min}^{-1}$ and the loading volume was 50 mL (equal to 25 mL of LV solution), which equaled 9.1×10^{11} total viral particles ($3.64 \times 10^{10} \text{ VP}\cdot\text{mL}^{-1}$) and 4.1×10^7 infectious viral particles ($1.64 \times 10^6 \text{ TU}\cdot\text{mL}^{-1}$). The ratio between physical particles compared to functional particles of the product was $2.2 \times 10^4 \text{ VP}\cdot\text{TU}^{-1}$.

At a constant PEG concentration of 12.5%, the LV particle recovery in the flow through fractions decreased significantly from $21 \pm 4\%$ to $1 \pm 0.5\%$ as the molecular weight of PEG increased (Fig. 5A). With a mixture of PEG 2000 and PEG 4000, the amount of LV lost in the flow through fractions is between the values measured for PEG 2000 and PEG 4000. This can be explained by the PEG-free depletion zone around the LV particles that becomes larger as the PEG size increases. Therefore, PEG 2000 (12.5%) led to twice as high LV particle loss in the flow through fraction compared with the mixtures of PEG 2000 and PEG 4000 having the same concentration. A different molar ratio with a higher proportion of PEG 4000 may result in less LV particle loss in flow through than with a molarity of 1:2. A higher PEG concentration is required to achieve the same depletion strength with smaller PEG sizes. The highest LV particle recovery in the elution was obtained for PEG 4000 ($86 \pm 18\%$). Using PEG 6000 at the same concentration, a significant drop in LV recovery ($p \leq 0.05$) in the elution fraction was observed ($52 \pm 2\%$). This is due to the viscoelastic properties of PEG 6000 as explained above. Fig. 5B shows overall high infectious virus particle recoveries ranging from 75% to 94% for different PEG molecular weights. Considering the error bars, the effect of the molecular weight of PEG on infectious LV recovery was negligible. The dsDNA and protein concentrations of the loading material were $477 \text{ ng}\cdot\text{mL}^{-1}$ and $241 \text{ }\mu\text{g}\cdot\text{mL}^{-1}$, respectively. Overall high protein and dsDNA removal between $77 \pm 4\%$ to $88 \pm 4\%$ was achieved (Fig. 5C), regardless of the PEG molecular weight used, which has been already discussed above.

Comparing our results of the investigation on the ideal PEG size and concentration to previous SXC studies, we observed a similar trend using PEG 4000 as described by Wang et al. [29] using PEG 6000: increased retention of the biomolecule of interest with increasing PEG concentration. However, it must be considered that γ -globulin is a small molecule (hydrodynamic radius 4.5 nm) compared with LVs and smaller molecules require larger PEG sizes to achieve efficient depletion retention. Other studies with viral vectors having a similar size like LV were performed and achieved an influenza A virus recovery of 83% with 8% PEG 6000 [25] and recovery above 90% of Orf virus with 8% PEG 8000 [30]. These findings do not agree with results obtained in our present study in which high recoveries were not obtained with PEG 6000 at a concentration ranging from 7.5% to 12.5% and a flow rate of $7 \text{ mL}\cdot\text{min}^{-1}$. However, it must be considered that a membrane device with a regenerated cellulose membrane with a pore size of $1 \text{ }\mu\text{m}$ (Whatman®) was used and the flow rate was set at $10 \text{ mL}\cdot\text{min}^{-1}$. Different process parameters, such as the flow rate or the specifications of the stationary phase used, can impact SXC performance. These different process parameters may explain why we observed optimal recoveries with different PEG buffers. Larger PEG sizes like PEG 8000 were not tested in our study due to pressure concerns, as discussed later in Section 3.4.

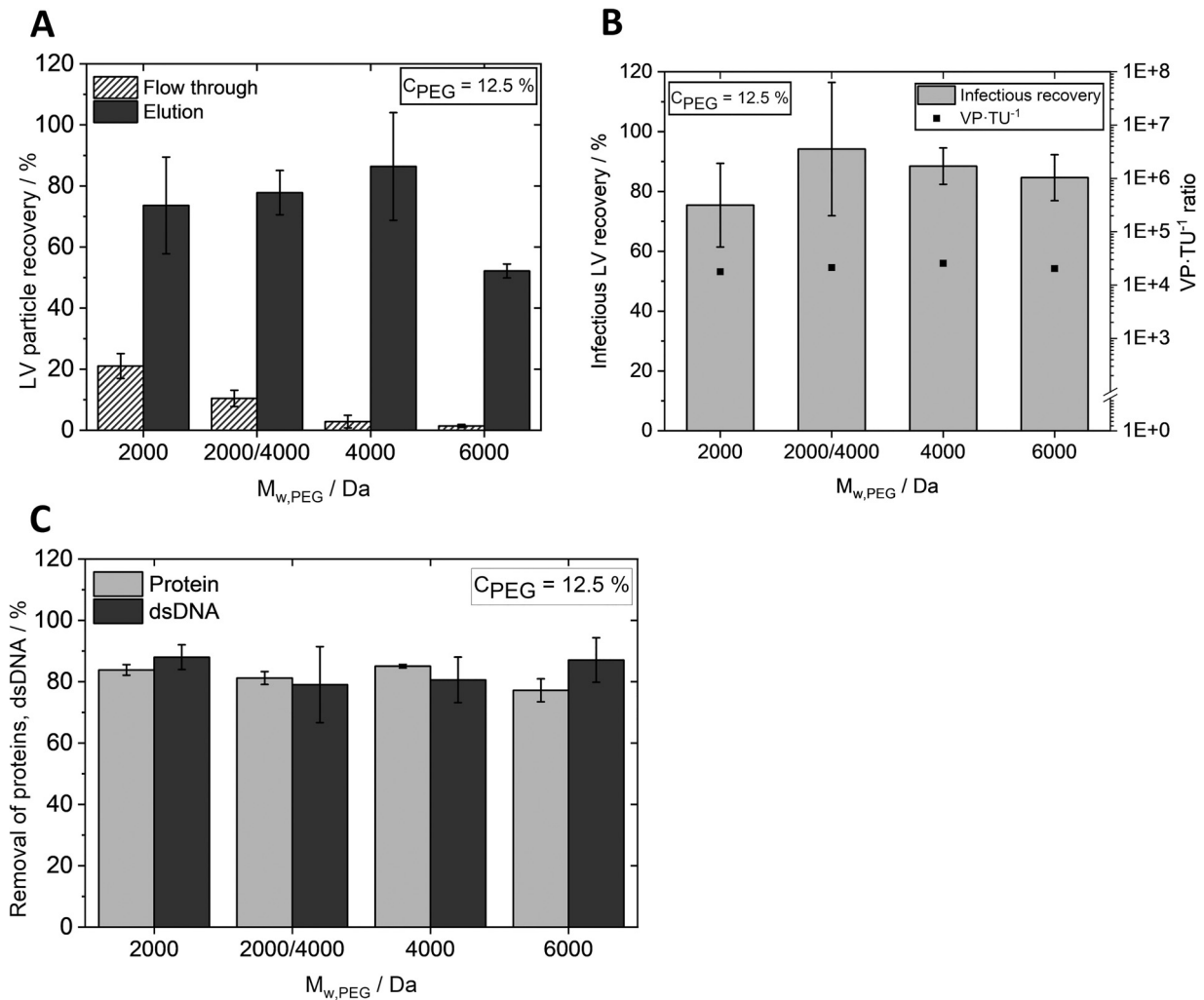


Fig. 5. LV titer recoveries and impurity removal using different PEG molecular weights at a constant PEG concentration. LV particle recovery in flow through and elution fractions (A), infectious LV recovery and viral particle to transducing unit ratio (VP·TU⁻¹) (B), and protein and dsDNA removal (C) plotted against the different molecular weights of PEG at a constant PEG concentration of 12.5%.

In terms of LV particle and infectious recovery, as well as impurity removal, the best results were achieved with PEG of a molecular weight of 4000 Da at a concentration of 12.5% using the 5-layer membrane device. The following experiments were performed with these parameters.

3.3. Optimal flow rate

To gain insight into the dynamic aspects of SXC, different flow rates were investigated to define an optimal flow rate at which high LV particle recoveries and infectious particle recoveries as well as high contaminant removal values are achieved. The purification step was performed systematically at flow rates of 3, 6, and 9 mL·min⁻¹. The flow rate was the same for all steps (loading, wash, elution). PEG 4000 at a final concentration of 12.5% and an SXC device with 5 membrane layers were used. An LV solution of 25 mL (equals 50 mL loading volume) was loaded, corresponding to 5.60×10^{12} total viral particles (2.24×10^{11} VP·mL⁻¹) and 9.25×10^7 infectious viral particles (3.70×10^6 TU·mL⁻¹). The ratio between physical particles compared to functional particles of the solution was 6.1×10^4 VP·TU⁻¹. The main effect plots obtained by MODDE Pro 13 in Fig. 6, depict the predicted values of the selected responses when the factor varies from low to high level. The experimental data (worksheet) is indicated in the plot as well.

LV particle recovery in the elution fraction increased significantly ($p \leq 0.001$) from $28 \pm 7\%$ to $75 \pm 11\%$ when the flow rate was increased from 3 mL·min⁻¹ to 6 mL·min⁻¹, but decreased significantly ($p \leq 0.05$) at a flow rate of 9 mL·min⁻¹ down to $47 \pm 9\%$ (Fig. 6A). LV particle recoveries in the wash and flow through fractions were below 4% for all runs (data not shown). A comparable trend was observed for infectious LV recovery, which increased significantly ($p \leq 0.001$) from $42 \pm 4\%$ to $79 \pm 5\%$ when the flow rate was increased from 3 mL·min⁻¹ to 6 mL·min⁻¹ and then decreased significantly ($p \leq 0.05$) to $61 \pm 8\%$ at a flow rate of 9 mL·min⁻¹ (Fig. 6D). The highest predicted LV particle recovery and infectious LV recovery are obtained for flow rates between 6 and 7 mL·min⁻¹. At a low flow rate, it takes more time for LV particles to reach the membrane of the chromatography device. It is possible that during this unfavorable state of free energy, self-association of the particles occurs before they reach the stationary phase. The subsequent elution of large aggregates is difficult. Another hypothesis is that the lower pressure at 3 mL·min⁻¹ was too low to reverse aggregation of the LV particles that bound to the membrane, thus challenging their proper elution. The residence time of LV particles in the stationary phase with 9 mL·min⁻¹ was possibly too short, hindering their retention. Moreover, at 9 mL·min⁻¹, the pressure limit was nearly reached, which is disadvantageous for the process. Lothert et al. [26] used the same membrane as

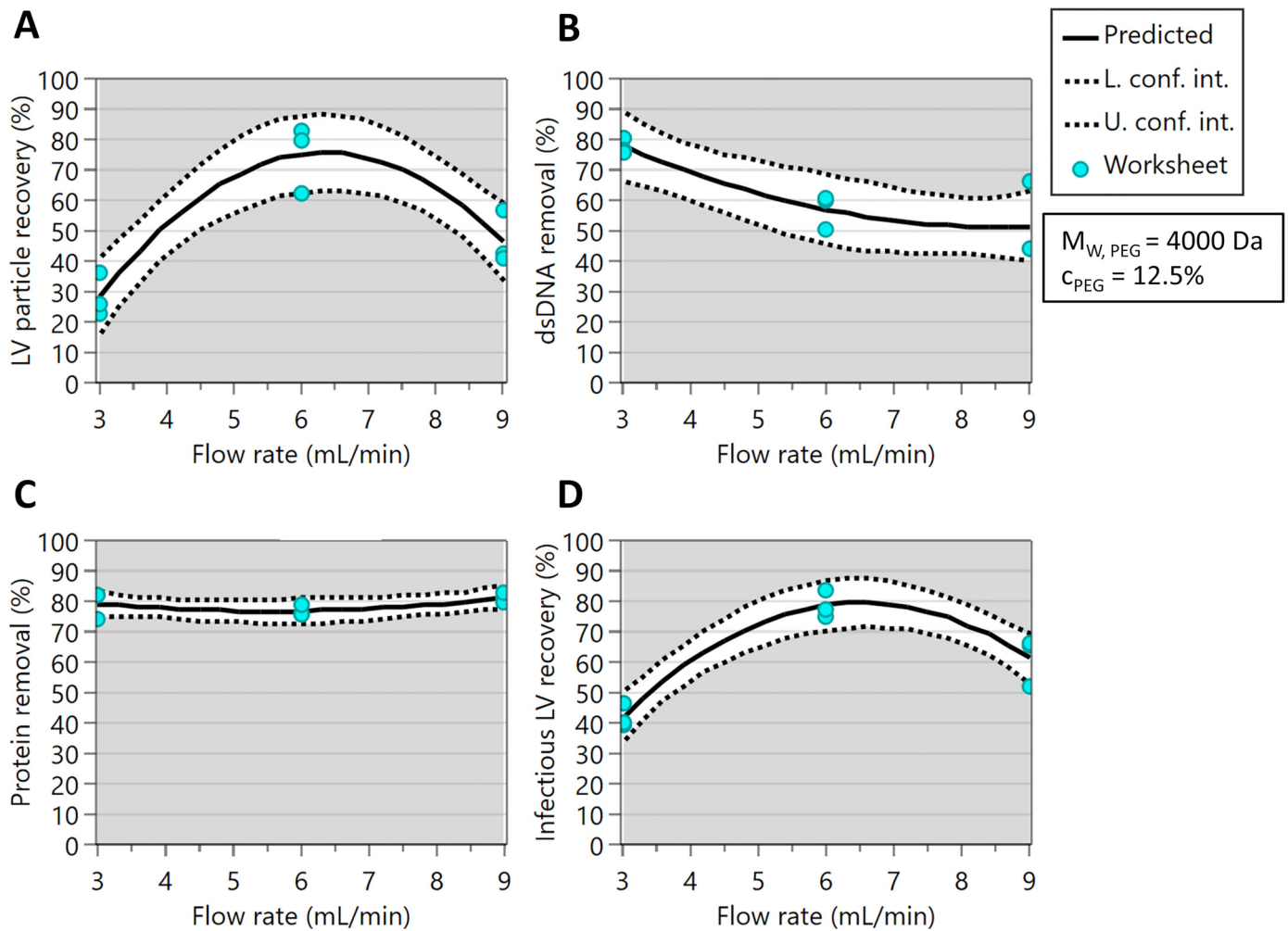


Fig. 6. Main effect plots of the flow rate. Predicted LV particle recovery (A), dsDNA removal (B), protein removal (C), and infectious LV recovery (D) for flow rates between 3 and 9 mL•min⁻¹. The measured data (worksheet) are displayed as blue dots. Solid lines show the predicted values; dotted lines, the lower and upper confidence intervals.

the one employed in our study as a stationary phase and observed that the flow rate had a high impact on virus retention and that the optimal flow rate depended on the PEG size and concentration used. We assert that optimal process conditions for flow rate and PEG buffer also depend on the stationary phase, e.g., membrane material, pore size, and thickness. Relatively high values of dsDNA and protein removal were obtained. A significant decrease in dsDNA removal ($p \leq 0.05$) from $78 \pm 2\%$ to $51 \pm 13\%$ was measured as the flow rate increased (Fig. 6B). The dsDNA removal rates at 6 mL•min⁻¹ and 9 mL•min⁻¹ did not significantly differ from one another ($p \leq 0.05$). Regardless of the flow rate, high protein removal values ranging from $77 \pm 2\%$ to $81 \pm 1\%$ were achieved (Fig. 6C). With respect to both LV recovery and impurity removal, a flow rate between 6 and 7 mL•min⁻¹ was defined as optimal.

3.4. Pressure profiles and maximum loading volumes for SXC

We hypothesized that pressure is a critical factor to consider when performing SXC, therefore we had a closer look at pressure profiles. In order to better understand which factors are the main drivers of pressure, we analyzed the pressures for various parameters, including different PEG buffers, flow rates, and loading volumes (Fig. 7A–C). The maximum pressure of the chromatography system was set to 0.6 MPa. The pre-column pressure was always around 0.17 MPa below the system pressure. The MALS detector

was not employed for these experiments as the use of this detector causes additional pressure that would have exceeded the maximum pressure under the conditions used.

The use of a lower molecular weight and concentration of PEG resulted in a lower viscosity of the PEG buffer which is reflected by the lower system pressure observed (Fig. 7A). PEG buffers are viscous, and as the viscosity and flow rate increase, the pressure rises (Fig. 7B). Lower pressures can be advantageous for extremely labile LV particles and the process itself. Therefore, smaller PEG sizes and lower PEG concentrations should be considered. PEG buffers with a molecular weight of greater than 6000 Da were thus excluded in this study. A polydisperse PEG buffer using a mixture of two different PEG molecular weights is an option when low operating pressures are required due to process limitations. A pressure profile for loading either 100 mL or 140 mL of the LV solution is shown in Fig. 7C. This profile indicates that the pressure continuously increased during the loading step, whereas it decreased rapidly during the elution step. As a pressure increase was observed during the loading step, the volume loaded, must also be considered to reduce operating pressure. We consider the amount of LV loaded is limited by the pressure increase during loading. We hypothesize that the pressure increase observed during loading occurs due to an increase in the amount of virus captured in the membrane, which leads to membrane fouling and, therefore, to a decrease in the membrane pore size. Consequently, operating SXC near the pressure limit is disadvantageous. A lower pressure,

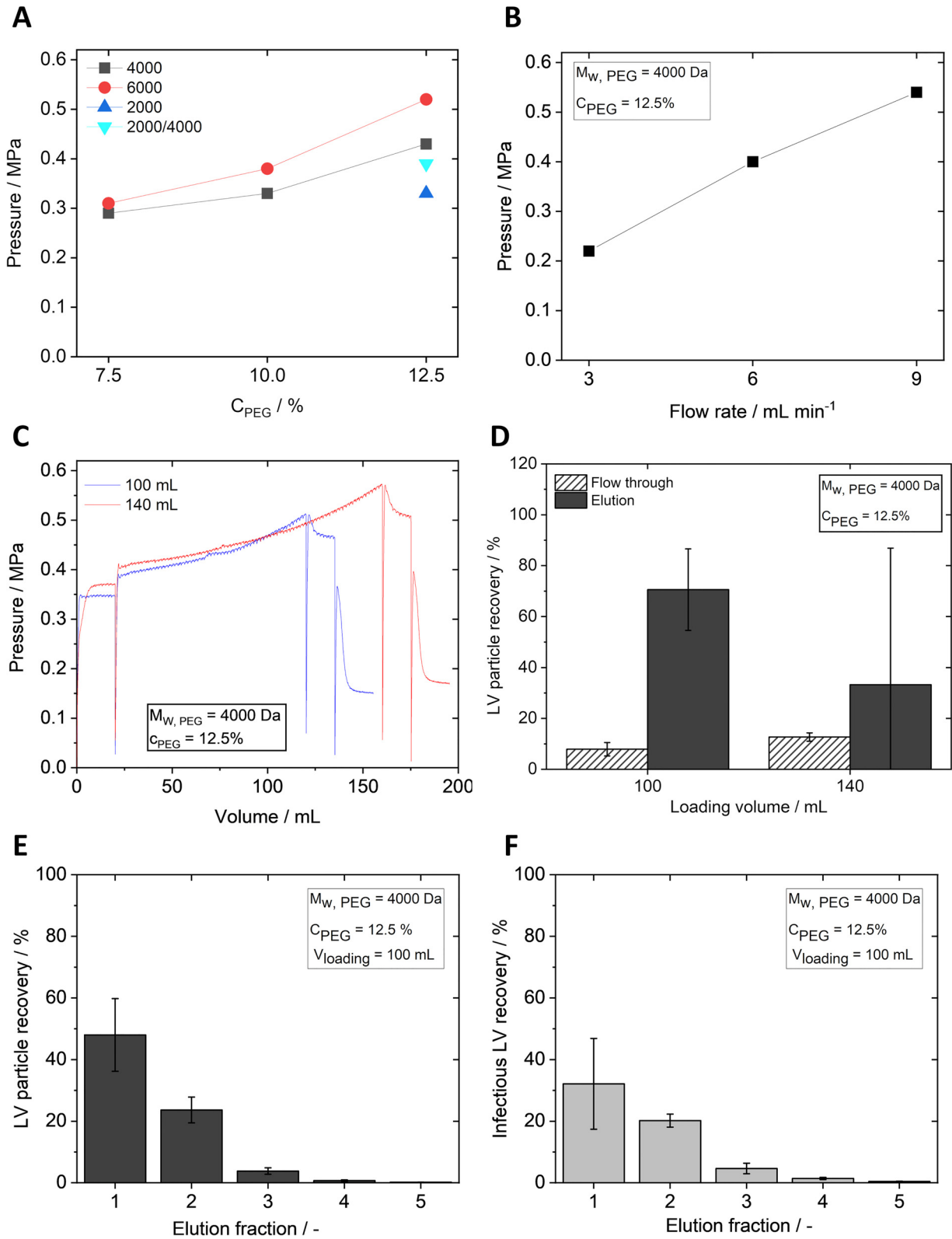


Fig. 7. Pressures and maximum loading volumes for SXC. System pressures during SXC runs using different PEG buffers (A), flow rates (B), and loading volumes (C). For A, B, the pressures at the end of the loading step are indicated. Recovered LV particles loading either 100 mL or 140 mL (equals 50 mL or 70 mL of LV solution loaded, respectively) (D). LV particle recovery (E) and infectious recovery (F) for the corresponding elution fraction loading of 100 mL (equals 50 mL LV solution). Each volume for the elution fractions was 10 mL.

achieved by selecting a suitable PEG buffer and an appropriate flow rate, would allow a higher number of loaded LV particles before the maximum pressure is reached.

In the next experiment, we investigated the effects of different loading volumes on LV recovery and determined the maximum loading capacity of the SXC device (Fig. 7D). The number of viral particles loaded was 7.5×10^{12} and 1.05×10^{13} total viral particles (1.50×10^{11} VP·mL⁻¹) for loading volumes of 100 mL and 140 mL (equals 50 mL and 70 mL LV solution), respectively. The LV particle recovery in the elution fraction was $71 \pm 16\%$ when 100 mL was loaded. When we attempted to load 140 mL, the pressure limit was reached at the end of the loading step for two of three replicates. The elution step, at which the pressure decreases, was performed for all runs, but only the elution of one out of three replicates was successful. While an LV particle recovery of 95% was obtained for the successfully eluted replicate, the two other replicates yielded an LV particle recovery of only 2–3%. Therefore, the LV particle recovery for the loading volume of 140 mL (Fig. 7D) shows an extremely high error bar. As it is not possible to elute LVs adequately after the maximum pressure has been reached, the membrane should not be overloaded. We hypothesize that when overloading the membrane aggregates are formed that block the membrane pores, thereby making it impossible to elute the viral particles as liquid flow through the membrane is restricted. Consequently, overloading the membrane and approaching the pressure limit hinders subsequent elution of the LV particles. Therefore, we recommend a maximum load of 7.5×10^{12} VP (in this case, 100 mL loading volume) per MA15 SXC 5-layer membrane device; with respect to the total available surface area of the device, the capacity is 3.06×10^{11} viral particles per cm². The pressure is of high importance, especially from a process perspective as maximum pressures of 0.3 to 0.4 MPa are typical for large-scale DSP processes, whereas the maximum pressure for the small-scale study was higher, at 0.6 MPa. This must be considered to scale up a purification process.

In a separate experiment we investigated the required elution volume when the loading volume was increased to 100 mL (3.42×10^{12} viral particles (6.84×10^{10} VP·mL⁻¹) and 9.57×10^7 infectious particles loaded (1.91×10^6 TU·mL⁻¹). The ratio between physical particles compared to functional particles of the product was 3.6×10^4 VP·TU⁻¹. Five elution fractions of 10 mL each were collected, and LV recovery was analyzed for each fraction separately (Fig. 7E and F) because the MALS detector could not be used, as described above. In the first and second fractions, LV particle recoveries of $48 \pm 12\%$ and $24 \pm 4\%$ were achieved. An LV particle recovery of 4% or below was obtained in the remaining fractions (Fig. 7E). In total, a particle recovery of $77 \pm 8\%$ was achieved across all elution fractions. An analog trend was observed for the infectious recovery as depicted in Fig. 7F. Infectious recovery values of $32 \pm 15\%$ and $20 \pm 2\%$ were achieved for the first and second elution fractions; infectious recovery values of 5% or below were obtained for the remaining fractions. In total, an infectious recovery of $59 \pm 16\%$ was achieved for all elution fractions. The LV particles and the infectious LV were mainly recovered in the first two to three elution fractions. Elution with 20 to 30 mL can therefore be considered sufficient for a 5-layer membrane SXC device. When collecting the first 20 mL of the eluate, a volumetric concentration factor of 2.5 of the LV was achieved. This is an advantage compared with AEX which includes typically a 5-fold dilution of the eluate to preserve the infectivity of LV and a subsequent feed volume reduction step [5,39,47] or an immediate desalting step after the elution step [48]. Some protocols even include a dilution of LV with loading buffer before AEX to meet the conductivity requirements of the method [39]. Thus, AEX chromatography results in higher buffer consumption and a weakened concentration of the LV [3]. We, therefore, regard it as an advantage that no pre or post-

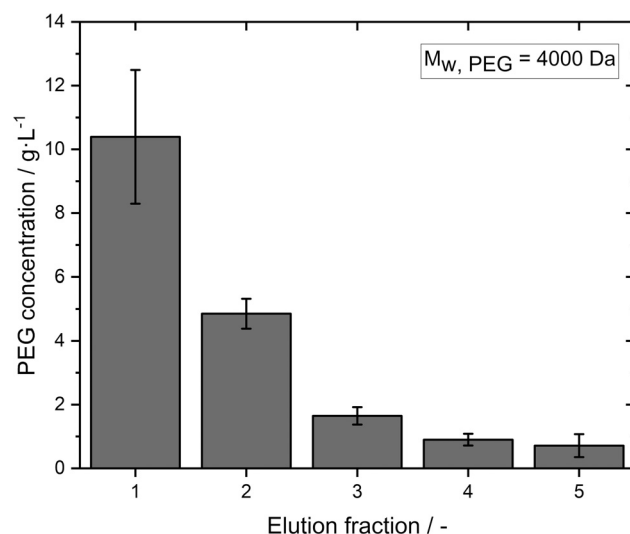


Fig. 8. PEG concentration in SXC elution fractions. PEG with a molecular weight of 4000 Da and 12.5% (w/v) was used to purify 100 mL of LV solution. The volume for each elution fraction was 10 mL.

treatment of the LV material is required for SXC as this simplifies and accelerates the downstream process.

3.5. Remaining PEG concentration in the eluate

The remaining PEG concentration in SXC eluate fractions is an important aspect to analyze since PEG poses immunogenicity concerns and should be cleared from the final drug product [53,54]. The PEG concentration of the SXC eluate was not determined in previous publications and is reported in this study for the first time. We analyzed the PEG 4000 concentration of five elution fractions of 10 mL each using a modified Dragendorff reagent. The PEG concentration decreased as the elution fraction increased (Fig. 8). Presumably, these are the PEG molecules that were contained in the dead volume of the device and were washed out as a result. For purification by SXC, two fractions (20 mL) were typically collected because most LV is recovered in these first two fractions, as depicted in Fig. 7E and 7F. For the first two fractions, this resulted in an average PEG concentration of 7.6 g·L⁻¹, which is about 6.1% of the PEG concentration used during loading; this corresponds to 152 mg PEG per 8.61×10^{11} viral particles. Since only about 6% of the starting PEG concentration was present in the first two fractions, this indicates that PEG does not bind to the membrane and is removed in the flow through and wash fractions. In this case, the biomolecules of interest, LV, are not PEGylated; some PEG is still present in the eluate and must be removed in subsequent DSP steps. Buffer exchange and concentration are typically performed after the purification step by ultrafiltration and diafiltration. Membranes with a molecular weight cut-off (MWCO) of 100 to 750 kDa [3] are used for LV concentration. The MWCO defines the lowest molecular weight at which more than 90% of the target molecule, in this case, the LV is retained. For viruses the molecular weight is not as relevant as diameter, therefore the best MWCO is given for the virus diameter [55]. Since PEG is about 20-times smaller compared to LV (2.5 nm gyration radius for PEG 4000 and 100 nm diameter for LV), it is expected that PEG is washed out in the permeate during ultrafiltration. For example, if retention of PEG is desired an MWCO of 1 kDa would be selected which is 100 to 750-times smaller than the MWCO employed for LV. It is preferable to select a smaller PEG size as it can be removed more easily as opposed to larger PEG sizes. For pharmaceutical purposes, the detection of residual PEG of the final product remains necessary.

4. Conclusion

The demand for efficient LV bioprocessing is increasing and emphasizes the need for downstream process strategies for fragile enveloped viral vectors like LV. The purification step is considered one of the main challenges due to the low stability of LV. SXC has great potential for overcoming the current bottleneck. In this study, we successfully identified optimal process parameters for SXC of lentiviral vector purification. The ideal process conditions for performing SXC to purify LV are 12.5% PEG 4000, and a flow rate between 6 and 7 mL·min⁻¹ for the specific membrane and device used in this study. Under these conditions, we achieved the highest LV particle recoveries and infectious recoveries of 86% and 88%, respectively. At the same time, high protein and dsDNA removal rates were observed at 81% and 79%, respectively. We defined the maximal loading capacity for the device used as 7.5×10^{12} lentiviral particles and showed that a concentration of the LV can be achieved when the first 20 mL of the eluate are collected. Moreover, we discussed pressure concerns in detail. The maximum pressure of the device and the pressure increase during loading must be considered during the selection of process parameters. Overloading the membrane is critical as adequate LV elution was not possible after the maximum pressure was reached. The remaining PEG concentration in the eluate was investigated. Further experiments are required to analyze the removal of the remaining PEG in the subsequent downstream processing steps. Given the results presented, SXC demonstrates a high potential for purification of LV and other enveloped viral vectors. A more in-depth mechanistic understanding of the SXC principle is required to develop a successful scale-up model of this method.

Declaration of Competing Interest

The authors declare that they have no known competing financial interests or personal relationships that could have appeared to influence the work reported in this paper.

CRediT authorship contribution statement

Jennifer J. Labisch: Conceptualization, Methodology, Investigation, Formal analysis, Visualization, Writing – original draft. **Meriem Kassar:** Methodology, Formal analysis, Writing – review & editing. **Franziska Bollmann:** Supervision, Writing – review & editing. **Angela Valentic:** Supervision, Writing – review & editing. **Jürgen Hubbuch:** Supervision. **Karl Pflanz:** Supervision, Project administration.

Acknowledgements

We would like to kindly thank Florian Hebenstreit for manufacturing the SXC membrane devices. We thank Philip Wiese for assistance with Fig. 1A. We thank Jutta Schippmann and Michael Metzke for providing scanning electron microscope pictures of the membrane (Fig. 1B and 1C).

References

- [1] John Wiley & Sons, IncGene Therapy Clinical Trials Worldwide, John Wiley & Sons, Inc, Hoboken, NJ, USA, 2021 Journal of Gene Medicine <https://a873679.fmphost.com/fmi/webd/GTCT> Accessed 11 November 2021.
- [2] J. Rininger, A. Fennell, L. Schoukroun-Barnes, C. Peterson, J. Speidel, Capacity analysis for viral vector manufacturing: is there enough? *BioProcess Int.* 17 (2019).
- [3] C. Perry, A.C.M.E. Rayat, Lentiviral vector bioprocessing, *Viruses* 13 (2021), doi:10.3390/v13020268.
- [4] A.S. Moreira, D.G. Cavaco, T.Q. Faria, P.M. Alves, M.J.T. Carrondo, C. Peixoto, Advances in lentivirus purification, *Biotechnol. J.* (2020) e2000019, doi:10.1002/biot.202000019.
- [5] M. Bauler, J.K. Roberts, C.C. Wu, B. Fan, F. Ferrara, B.H. Yip, S. Diao, Y.I. Kim, J. Moore, S. Zhou, M.M. Wielgosz, B. Ryu, R.E. Throm, Production of lentiviral vectors using suspension cells grown in serum-free media, *Mol. Ther. Methods Clin. Dev.* 17 (2020) 58–68, doi:10.1016/j.omtm.2019.11.011.
- [6] A.J. Valkama, I. Oruetebarria, E.M. Lippinen, H.M. Leinonen, P. Käyhty, H. Hynynen, V. Turkki, J. Malinen, T. Miinalainen, T. Heikura, N.R. Parker, S. Ylä-Herttua, H.P. Lesch, Development of large-scale downstream processing for lentiviral vectors, *Mol. Ther. Methods Clin. Dev.* 17 (2020) 717–730, doi:10.1016/j.omtm.2020.03.025.
- [7] H.B. Olgun, H.M. Tasyurek, A.D. Sanlioglu, S. Sanlioglu, High-grade purification of third-generation HIV-based lentiviral vectors by anion exchange chromatography for experimental gene and stem cell therapy applications, *Methods Mol. Biol.* 1879 (2019) 347–365, doi:10.1007/978-1-4939-9065-8_8.
- [8] S. Tinch, K. Szczur, W. Swaney, L. Reeves, S.R. Witting, A scalable lentiviral vector production and purification method using Mustang Q chromatography and tangential flow filtration, *Methods Mol. Biol.* 1937 (2019) 135–153, doi:10.1007/978-1-4939-9065-8_8.
- [9] A.S. Moreira, T.Q. Faria, J.G. Oliveira, A. Kavara, M. Schofield, T. Sanderson, M. Collins, R. Gantier, P.M. Alves, M.J.T. Carrondo, C. Peixoto, Enhancing the purification of lentiviral vectors for clinical applications, *Sep. Purif. Technol.* 274 (2021) 118598, doi:10.1016/j.seppur.2021.118598.
- [10] M. Segura, A. Kamen, P. Trudel, A. Garnier, A novel purification strategy for retrovirus gene therapy vectors using heparin affinity chromatography, *Biotechnol. Bioeng.* 90 (2005) 391–404, doi:10.1002/bit.20301.
- [11] M.M. Segura, A. Garnier, Y. Durocher, H. Coelho, A. Kamen, Production of lentiviral vectors by large-scale transient transfection of suspension cultures and affinity chromatography purification, *Biotechnol. Bioeng.* 98 (2007) 789–799, doi:10.1002/bit.21467.
- [12] M. Zhao, M. Vandersluis, J. Stout, U. Haupts, M. Sanders, R. Jacquemart, Affinity chromatography for vaccines manufacturing: finally ready for prime time? *Vaccine* 37 (2019) 5491–5503, doi:10.1016/j.vaccine.2018.02.090.
- [13] K. Ye, S. Jin, M.M. Atai, J.S. Schultz, J. Ibeh, Tagging retrovirus vectors with a metal binding peptide and one-step purification by immobilized metal affinity chromatography, *J. Virol.* 78 (2004) 9820–9827, doi:10.1128/JVI.78.18.9820-9827.2004.
- [14] M.C. Cheeks, N. Kamal, A. Sorrell, D. Darling, F. Farzaneh, N.K.H. Slater, Immobilized metal affinity chromatography of histidine-tagged lentiviral vectors using monolithic adsorbents, *J. Chromatogr. A* 1216 (2009) 2705–2711, doi:10.1016/j.chroma.2008.08.029.
- [15] J.H. Yu, D.V. Schaffer, Selection of novel vesicular stomatitis virus glycoprotein variants from a peptide insertion library for enhanced purification of retroviral and lentiviral vectors, *J. Virol.* 80 (2006) 3285–3292, doi:10.1128/JVI.80.7.3285-3292.2006.
- [16] R. Chen, N. Folarin, V.H.B. Ho, D. McNally, D. Darling, F. Farzaneh, N.K.H. Slater, Affinity recovery of lentivirus by diaminoethylamine mediated desthiobiotin labelling, *J. Chromatogr. B Anal. Technol. Biomed. Life Sci.* 878 (2010) 1939–1945, doi:10.1016/j.jchromb.2010.05.019.
- [17] L. Mekkaoui, F. Parekh, E. Kotsopoulou, D. Darling, G. Dickson, G.W. Cheung, L. Chan, K. MacLellan-Gibson, G. Mattiuzzo, F. Farzaneh, Y. Takeuchi, M. Pule, Lentiviral vector purification using genetically encoded biotin mimic in packaging cell, *Mol. Ther. Methods Clin. Dev.* 11 (2018) 155–165, doi:10.1016/j.omtm.2018.10.008.
- [18] F. Higashikawa, L. Chang, Kinetic analyses of stability of simple and complex retroviral vectors, *Virology* 280 (2001) 124–131, doi:10.1006/viro.2000.0743.
- [19] J.J. Labisch, G.P. Wiese, K. Barnes, F. Bollmann, K. Pflanz, Infectious titer determination of lentiviral vectors using a temporal immunological real-time imaging approach, *PLoS ONE* 16 (2021) e0254739, doi:10.1371/journal.pone.0254739.
- [20] O.W. Merten, M. Schweizer, P. Chahal, A. Kamen, Manufacturing of viral vectors: part II. Downstream processing and safety aspects, *Pharm. Bioprocess.* 2 (2014) 237–251, doi:10.4155/PBP.14.15.
- [21] S.L. Williams, D. Nesbeth, D.C. Darling, F. Farzaneh, N.K.H. Slater, Affinity recovery of moloney murine leukaemia virus, *J. Chromatogr. B Anal. Technol. Biomed. Life Sci.* 820 (2005) 111–119, doi:10.1016/j.jchromb.2005.03.016.
- [22] T. Rodrigues, M.J.T. Carrondo, P.M. Alves, P.E. Cruz, Purification of retroviral vectors for clinical application: biological implications and technological challenges, *J. Biotechnol.* 127 (2007) 520–541, doi:10.1016/j.jbiotec.2006.07.028.
- [23] J. Lee, H.T. Gan, S.M.A. Latiff, C. Chuah, W.Y. Lee, Y.S. Yang, B. Loo, S.K. Ng, P. Gagnon, Principles and applications of steric exclusion chromatography, *J. Chromatogr. A* 1270 (2012) 162–170, doi:10.1016/j.chroma.2012.10.062.
- [24] P. Gagnon, P. Toh, J. Lee, High productivity purification of immunoglobulin G monoclonal antibodies on starch-coated magnetic nanoparticles by steric exclusion of polyethylene glycol, *J. Chromatogr. A* 1324 (2013) 171–180, doi:10.1016/j.chroma.2013.11.039.
- [25] P. Marichal-Gallardo, M.M. Pieler, M.W. Wolff, U. Reichl, Steric exclusion chromatography for purification of cell culture-derived influenza A virus using regenerated cellulose membranes and polyethylene glycol, *J. Chromatogr. A* 1483 (2017) 110–119, doi:10.1016/j.chroma.2016.12.076.
- [26] K. Lothert, G. Sprick, F. Beyer, G. Lauria, P. Czeremak, M.W. Wolff, Membrane-based steric exclusion chromatography for the purification of a recombinant baculovirus and its application for cell therapy, *J. Virol. Methods* 275 (2020) 113756, doi:10.1016/j.jviromet.2019.113756.
- [27] K. Lothert, F. Pagallies, T. Feger, R. Amann, M.W. Wolff, Selection of chromatographic methods for the purification of cell culture-derived Orf virus for its application as a vaccine or viral vector, *J. Biotechnol.* 323 (2020) 62–72, doi:10.1016/j.jbiotec.2020.07.023.

- [28] P. Marichal-Gallardo, K. Börner, M.M. Pieler, V. Sonntag-Buck, M. Obr, D. Bejarano, M.W. Wolff, H.G. Kräusslich, U. Reichl, D. Grimm, Single-use capture purification of adeno-associated viral gene transfer vectors by membrane-based steric exclusion chromatography, *Hum. Gene Ther.* 32 (2021) 959–974, doi:10.1089/hum.2019.284.
- [29] C. Wang, S. Bai, S.P. Tao, Y. Sun, Evaluation of steric exclusion chromatography on cryogel column for the separation of serum proteins, *J. Chromatogr. A* 1333 (2014) 54–59, doi:10.1016/j.chroma.2014.01.059.
- [30] K. Lothert, F. Pagallies, F. Eilts, A. Sivanapillai, M. Hardt, A. Moebus, T. Feger, R. Amann, M.W. Wolff, A scalable downstream process for the purification of the cell culture-derived Orf virus for human or veterinary applications, *J. Biotechnol.* 323 (2020) 221–230, doi:10.1016/j.jbiotec.2020.08.014.
- [31] S. Asakura, F. Oosawa, On interaction between two bodies immersed in a solution of macromolecules, *J. Chem. Phys.* 22 (1954) 1255–1256, doi:10.1063/1.1740347.
- [32] A. Vrij, Polymers at interfaces and the interactions in colloidal dispersions, *Pure Appl. Chem.* 4 (1976) 471–483, doi:10.1351/pac197648040471.
- [33] Q. He, Investigation of stabilization mechanisms for colloidal suspension using nanoparticles. Electronic Theses and Dissertations, 2014. 10.18297/etd/593.
- [34] H.N.W. Lekkerkerker, R. Tuinier, *Colloids and the Depletion Interaction*, Springer, Netherlands, Dordrecht, 2011, doi:10.1007/978-94-007-1223-2.
- [35] R. Tuinier, J. Rieger, C.G. de Kruijf, Depletion-induced phase separation in colloid–polymer mixtures, *Adv. Colloid Interface Sci.* 103 (2003) 1–31, doi:10.1016/S0001-8686(02)00081-7.
- [36] J.J. Labisch, F. Bollmann, M.W. Wolff, K. Pflanz, A new simplified clarification approach for lentiviral vectors using diatomaceous earth improves throughput and safe handling, *J. Biotechnol.* (2021) 11–20, doi:10.1016/j.jbiotec.2020.12.004.
- [37] J.A. Tolk, *Mikrofiltrationsmembranen Auf Basis regenerierter Cellulose*. Dissertation, Hannover, 2017.
- [38] P. Escarpe, N. Zayek, P. Chin, F. Borellini, R. Zufferey, G. Veres, V. Kiermer, Development of a sensitive assay for detection of replication-competent recombinant lentivirus in large-scale HIV-based vector preparations, *Mol. Ther.* 8 (2003) 332–341, doi:10.1016/S1525-0016(03)00167-9.
- [39] J. Ruscic, C. Perry, T. Mukhopadhyay, Y. Takeuchi, D.G. Bracey, Lentiviral vector purification using nanofiber ion-exchange chromatography, *Mol. Ther. Methods Clin. Dev.* 15 (2019) 52–62, doi:10.1016/j.omtm.2019.08.007.
- [40] K. Lothert, A.F. Offersgaard, A.F. Pihl, C.K. Mathiesen, T.B. Jensen, G.P. Alzua, U. Fahne, J. Bukh, J.M. Gottwein, M.W. Wolff, Development of a downstream process for the production of an inactivated whole hepatitis C virus vaccine, *Sci. Rep.* 10 (2020) 16261, doi:10.1038/s41598-020-72328-5.
- [41] M.D. Hein, H. Kollmus, P. Marichal-Gallardo, S. Püttker, D. Benndorf, Y. Genzel, K. Schughart, S.Y. Kupke, U. Reichl, OP7, a novel influenza A virus defective interfering particle: production, purification, and animal experiments demonstrating antiviral potential, *Appl. Microbiol. Biotechnol.* 105 (2021) 129–146, doi:10.1007/s00253-020-11029-5.
- [42] F. Matter, A.L. Luna, M. Niederberger, From colloidal dispersions to aerogels: how to master nanoparticle gelation, *Nano Today* 30 (2020) 100827, doi:10.1016/j.nantod.2019.100827.
- [43] M. Baumgaertel, N. Willenbacher, The relaxation of concentrated polymer solutions, *Rheol. Acta* 35 (1996) 168–185, doi:10.1007/BF00396044.
- [44] M.Z. Jora, M.V.C. Cardoso, E. Sabadini, Dynamical aspects of water-poly(ethylene glycol) solutions studied by ¹H NMR, *J. Mol. Liq.* 222 (2016) 94–100, doi:10.1016/j.molliq.2016.06.101.
- [45] G. Böhme, *Strömungsmechanik Nichtnewtonscher Fluide*, 2nd ed., Vieweg+Teubner Verlag, Wiesbaden, 2000, doi:10.1007/978-3-322-80140-1.
- [46] M. Rubinstein, R.H. Colby, *Polymer Physics*, Oxford Univ. Press, Oxford, 2014.
- [47] V. Bandeira, C. Peixoto, A.F. Rodrigues, P.E. Cruz, P.M. Alves, A.S. Coroadinha, M.J.T. Carrondo, Downstream processing of lentiviral vectors: releasing bottle-necks, *Hum. Gene Ther. Methods* 23 (2012) 255–263, doi:10.1089/hgtb.2012.059.
- [48] R.H. Kutner, S. Puthli, M.P. Marino, J. Reiser, Simplified production and concentration of HIV-1-based lentiviral vectors using HYPERFlask vessels and anion exchange membrane chromatography, *BMC Biotechnol.* 9 (2009), doi:10.1186/1472-6750-9-10.
- [49] S.S. Rane, R.J. Dearman, I. Kimber, S. Uddin, S. Bishop, M. Shah, A. Podmore, A. Pluen, J.P. Derrick, Impact of a heat shock protein impurity on the immunogenicity of biotherapeutic monoclonal antibodies, *Pharm. Res.* 36 (2019) 51, doi:10.1007/s11095-019-2586-7.
- [50] B. Alberts, A. Johnson, J. Lewis, D. Morgan, M. Raff, K. Roberts, P. Walter, *Molecular Biology of the Cell*, 6th ed., Garland Science, New York, 2015.
- [51] O.-W. Merten, S. Charrier, N. Laroudie, S. Fauchille, C. Dugué, C. Jenny, M. Audit, M.A. Zanta-Boussif, H. Chautard, M. Radrizzani, G. Vallanti, L. Naldini, P. Noguez-Hellin, A. Galy, Large-scale manufacture and characterization of a lentiviral vector produced for clinical *ex vivo* gene therapy application, *Hum. Gene Ther.* 22 (2011) 343–356, doi:10.1089/hum.2010.060.
- [52] S. Yang, H. Tan, D. Yan, E. Nies, A.C. Shi, Effect of polydispersity on the depletion interaction in nonadsorbing polymer solutions, *Phys. Rev. E Stat. Nonlinear Soft Matter Phys.* 75 (2007) 61803, doi:10.1103/PhysRevE.75.061803.
- [53] N. d'Avanzo, C. Celia, A. Barone, M. Carafa, L. Di Marzio, H.A. Santos, M. Fresta, Immunogenicity of polyethylene glycol based nanomedicines: mechanisms, clinical implications and systematic approach, *Adv. Ther.* 3 (2020) 1900170, doi:10.1002/adtp.201900170.
- [54] M. Swierczewska, K.C. Lee, S. Lee, What is the future of PEGylated therapies? *Expert Opin. Emerg. Drugs* 20 (2015) 531–536, doi:10.1517/14728214.2015.1113254.
- [55] R. Singh, *Membrane Technology and Engineering for Water Purification* (Second Edition), in: *Application, Systems Design and Operation*, 2015, pp. 1–80, doi:10.1016/B978-0-444-63362-0.00001-X.